

## Insights into the Nature of Synergistic Effects in Proton-Conducting 4,4-1*H*,1*H*-Bitriazole-Poly(ethylene oxide) Composites

Christopher A. Alabi,<sup>†</sup> Zhongwei Chen,<sup>‡,§</sup> Yushan S. Yan,<sup>‡</sup> and Mark E. Davis<sup>\*,†</sup>

<sup>†</sup>Division of Chemistry and Chemical Engineering, California Institute of Technology, 1200 East California Boulevard, MC 210-41, Pasadena, California 91125, and <sup>‡</sup>Department of Chemical and Environmental Engineering, University of California, Riverside, California 92521. <sup>§</sup>Current address: University of Waterloo

Received June 24, 2009. Revised Manuscript Received August 25, 2009

A nitrogen-containing heterocycle (NCH), 4,4-1*H*-1*H*-bi-1,2,3-triazole (bitriazole), capable of mimicking the hydrogen bonding of water in the solid state is synthesized and its ability to conduct protons in the presence of poly(ethylene oxides) under anhydrous conditions is investigated. Bitriazole is shown to have sufficient thermal and electrochemical stability for fuel cell applications. The composites formed between bitriazole and poly(ethylene oxides) give proton conductivities that can be described by the Vogel–Tamman–Fulcher (VTF) equation. These characteristics suggest coupling between polymer segmental motion and ion transport. The bitriazole N-*H* proton is shown to be the source of conductivity, and bitriazole and poly(ethylene oxides) function synergistically through specific intermolecular interactions and polymer-induced segmental motion to create a pathway for proton transport via structural diffusion.

### Introduction

Solid proton conductors are a class of solid electrolytes that can conduct hydrogen ions via several transport mechanisms: structural diffusion, vehicular transport, and tunneling. These solid electrolytes are an essential part of several devices such as sensors, batteries, and fuel cells. The efficient operation and widespread commercial use of fuel cells, in particular, the hydrogen proton exchange membrane fuel cell, hinges on the development of low-cost proton conductors that can operate at both low and intermediate temperatures (120–180 °C) under dry (nonhumidified) conditions with high conductivities. Fuel cell operation at intermediate temperatures results in faster kinetics at the electrodes and lower overall fuel-cell costs. The latter is due to a reduction in the required platinum loading. Current solid electrolyte membranes such as Nafion and other acidic polymers are based on incorporation of strong hydrophilic Brønsted acids onto different hydrophobic polymer backbones. In spite of their excellent conductivities below the dew point of water, their dependence on the degree of hydration, through which they attain fast proton mobility, limits their performance under preferred fuel cell working conditions of intermediate temperatures and low humidity.

As an alternative approach, the use of amphoteric NCHs as the proton conducting species has been proposed by Kreuer.<sup>1,2</sup> These compounds mimic water with respect to their hydrogen-bonding capabilities and amphoteric nature. Several monomeric NCHs (Table 1) and

polymeric NCH blends with acids<sup>3–9</sup> have been reported. Studies carried out with imidazole,<sup>10,11</sup> triazole,<sup>9,12</sup> benzimidazole,<sup>13</sup> and pyrazoles<sup>2</sup> as the proton conducting groups have revealed that the proton conductivity of these NCHs depends on two factors. One factor is local mobility that can be achieved by heating the NCHs close to their melting points where high mobility is realized, or by tethering the NCHs to flexible polymer backbones whereby conductivity is governed by the flexibility of the polymer matrix. Tethering is preferred because it reduces the potential for leaching or evaporative loss of the small monomeric components from the blended mixture, especially at high temperatures (> 120 °C) where most NCHs liquefy. A second factor involves the effective concentrations of mobile protons, i.e., charge carrier density, which plays a larger role at higher temperatures where mobility of the NCHs is no longer an issue. The effective charge carrier density is a function of the acidity/basicity of the NCH group and the number density of the tethered

\*Corresponding author. E-mail: mdavis@cheme.caltech.edu.

(1) Kreuer, K. D. *Solid State Ionics* 1997, 94(1–4), 55–62.

(2) Kreuer, K. D.; Fuchs, A.; Ise, M.; Spaeth, M.; Maier, J. *Electrochim. Acta* 1998, 43(10–11), 1281–1288.

(3) Bozkurt, A.; Meyer, W. H.; Wegner, G. *J. Power Sources* 2003, 123(2), 126–131.

(4) Li, S. W.; Zhou, Z.; Zhang, Y. L.; Liu, M. L.; Li, W. *Chem. Mater.* 2005, 17(24), 5884–5886.

(5) Liu, Y. F.; Yu, Q. C.; Yuan, J.; Ma, L. L.; Wu, Y. H. *Eur. Polym. J.* 2006, 42(9), 2199–2203.

(6) Pu, H. T.; Liu, G. H. *Polym. Adv. Technol.* 2004, 15(12), 726–730.

(7) Yamada, M.; Honma, I. *Polymer* 2004, 45(25), 8349–8354.

(8) Yamada, M.; Honma, I. *Polymer* 2005, 46(9), 2986–2992.

(9) Zhou, Z.; Li, S. W.; Zhang, Y. L.; Liu, M. L.; Li, W. *J. Am. Chem. Soc.* 2005, 127(31), 10824–10825.

(10) Schuster, M.; Meyer, W. H.; Wegner, G.; Herz, H. G.; Ise, M.; Schuster, M.; Kreuer, K. D.; Maier, J. *Solid State Ionics* 2001, 145(1–4), 85–92.

(11) Schuster, M. F. H.; Meyer, W. H.; Schuster, M.; Kreuer, K. D. *Chem. Mater.* 2004, 16(2), 329–337.

(12) Subbaraman, R.; Ghassemi, H.; Zawodzinski, T. A. *J. Am. Chem. Soc.* 2007, 129(8), 2238–.

(13) Persson, J. C.; Jannasch, P. *Chem. Mater.* 2003, 15(16), 3044–3045.

Table 1. Chemical Properties of NCHs and Water

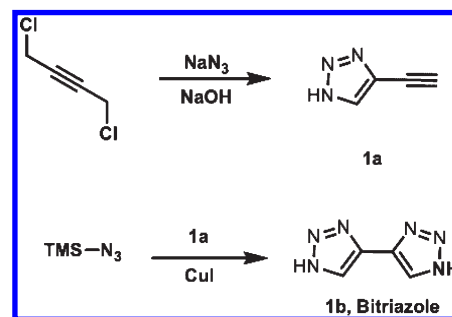
molecule	mp	acidic $pK_a$	basic $pK_a$	hydrogen-bond (total)
water	0	15.7	-1.7	4
imidazole	90	14.1	7.2	2
benzimidazole	178	12.6	5.7	2
1,2,3-triazole	23	8.7	1.5	3
1,2,4-triazole	120	9.9	2.4	3
bitriazole	210 <sup>a</sup>	6.4 <sup>b</sup>	-1 <sup>b</sup>	6

<sup>a</sup>Decomposition temperature. <sup>b</sup>Calculated according to Advanced Chemistry Development (ACD/Laboratories) Software V8.19.

groups. Li and co-workers evaluated the effect of reducing the  $pK_a$  of the NCH group and found that increasing the acidity of the NCH results in an appreciable increase in proton conductivity.<sup>4,9</sup>

Through careful design and adoption of these two basic principles, i.e., mobility and charge density, anhydrous proton conductivity has been realized in several polymeric-NCHs, where the NCHs have been tethered either by alkyl chains or by short poly(ethylene oxide) (PEO) spacers. Schuster et al. studied proton transport in imidazole-terminated ethylene oxide (EO) oligomers as model immobilized materials and found structural diffusion to be the dominant conduction process by comparing conductivity values to <sup>1</sup>H NMR diffusion coefficients.<sup>10,11</sup> Subsequently, Hertz et al. investigated two polymeric systems: imidazoles tethered to polystyrene and benzimidazole tethered to a polysiloxane network.<sup>14</sup> Higher conductivities were observed in the former because of improved polymer mobility. Persson and Jannasch studied the proton conductivity in benzimidazole-tethered ABA-PEO triblock copolymers and found conductivity to be promoted by high benzimidazole concentrations and high segmental mobilities.<sup>15,16</sup> These two factors were at odds with each other as higher benzimidazole concentrations led to more rigid (higher glass transition temperatures ( $T_g$ )) polymers. This result was further highlighted with benzimidazole containing poly(ethylene glycol) (PEG)-acrylates synthesized by Woudenberg et al.<sup>17</sup> Here, it was found that decreasing  $T_g$  by increasing the PEG content in the polymer led to enhanced conductivities at low temperatures and converging conductivities at higher temperatures (where the  $T_g$  of the parent polymer was surpassed). The conductivities converged at higher temperatures due to a decrease in charge carrier density as the volume fraction of the PEG increased. However, when the heterocycle was switched to a triazole,<sup>18</sup> an increase in PEG composition led to an increase in conductivity at all temperatures, and implies an improvement in conductivity despite a reduction in proton

Scheme 1. Synthesis of Bitriazole



carrier density. The authors mentioned the possibility of a synergistic effect and suggested that the dielectric constant of the PEG could have a positive influence on the conductivity as seen in lithium conducting polymer systems.

The objective of our work is to investigate and gain a fundamental understanding of the origin and mechanism of proton conductivity in a NCH-polymer composite in order to aid the design of future anhydrous organic-based proton electrolyte membranes. Here, we chose to decouple the polymer from the NCH so as to clearly study intermolecular polymer-NCH interactions. To do this, we synthesized 4,4-1*H*-1*H*-bi-1,2,3-triazole (bitriazole), a stable NCH capable of mimicking the hydrogen bonding of water in the solid state and studied its proton conductivity in the presence of different polymers. The source of proton conductivity in the bitriazole-poly(ethylene oxide) composites is revealed and a Grotthuss (structural diffusion) mechanism of proton transport is proposed based on our experimental findings. In addition, evidence of synergistic effects between bitriazole and poly(ethylene oxide) (PEO) as they relate to anhydrous proton conductivity enhancement is discussed.

## Experimental Section

**Materials.** Sodium azide, copper iodide, trimethylsilyl azide, polyethylene glycol dimethyl ether (PEO,  $M_n \approx 1000$ , 4000, and 8000 g/mol), polyethylene glycol (PEG,  $M_n \approx 1000$ ), polypropylene glycol (PPG,  $M_n \approx 1000$ ), and polyethylene glycol dithiol ( $M_w \approx 1500$ ) were purchased from Sigma-Aldrich and used as received. Poly(ethylene oxide) dicarboxylic acid was purchased from Quanta Biodesign. 1,4-Dichlorobut-2-yne was purchased and used as received from Alfa Aesar. All solvents were purified by fractional distillation from the appropriate drying agents or dried by filtration through the appropriate drying agents prior to use.

**Preparation of Bitriazole and Bitriazole-PEO Composites.** Bitriazole is synthesized in two steps from 1,4-dichlorobut-2-yne via 4-ethynyl-1*H*-1,2,3-triazole (**1a**) as an intermediate as shown in Scheme 1. The intermediate, **1a**, is formed via an azabutatriene type rearrangement after addition of sodium azide to 1,4-dichlorobut-2-yne. Compound **1b** is obtained from **1a** via “click chemistry” with a trimethylsilyl protected azide which undergoes deprotection in situ. Compound **1b**, i.e., the bitriazole, is obtained after sublimation as a crystalline white solid. Bitriazole-PEO composites were prepared as follows. The desired ratio of 4,4-1*H*,1*H*-1,2,3-bitriazole to poly(ethylene oxide) was dissolved in anhydrous methanol. Poly(ethylene oxide),

(14) Herz, H. G.; Kreuer, K. D.; Maier, J.; Scharfenberger, G.; Schuster, M. F. H.; Meyer, W. H. *Electrochim. Acta* **2003**, *48*(14–16), 2165–2171.

(15) Persson, J. C.; Jannasch, P. *Solid State Ionics* **2006**, *177*(7–8), 653–658.

(16) Persson, J. C.; Jannasch, P. *Chem. Mater.* **2006**, *18*(13), 3096–3102.

(17) Woudenberg, R. C.; Yavuzetin, O.; Tuorninen, M. T.; Coughlin, E. B. *Solid State Ionics* **2007**, *178*(15–18), 1135–1141.

(18) Martwiset, S.; Woudenberg, R. C.; Granados-Focil, S.; Yavuzetin, O.; Tuominen, M. T.; Coughlin, E. B. *Solid State Ionics* **2007**, *178*, 1398–1403.

$M_n \approx 1000$  was used unless stated otherwise. The mixture was heated for a few minutes to ensure complete dissolution and stirred at room temperature for another 15 min. Methanol was then removed and the resulting solid was dried for 3 h under vacuo (500 mTorr). Twenty milligrams of the dried solid was weighed out, placed in a 6.1 mm die set sandwiched between two platinum blocking electrodes (6 mm circular plates), and pressed at 2000 lbs for 1–2 min. Average pellet thickness fell between 100 and 300  $\mu\text{m}$ .

**Characterization.**  $^1\text{H}$  and  $^{13}\text{C}$  liquid NMR (300 MHz) spectra were obtained on a Varian Mercury-300 NMR Spectrometer with samples dissolved in either *d*-chloroform or *d*-dimethylsulfoxide ( $\text{DMOS-d}_6$ ).  $^1\text{H}$  and  $^{13}\text{C}$  solid-state CP MAS NMR spectra were recorded at 10–13 kHz using a Bruker Avance 500 MHz spectrometer with a 4 mm rotor. Thermogravimetric analyses (TGA) were performed on a Netzsch STA 449 C with Pt/Rh crucibles. The samples were heated under argon or air at a heating rate of 10  $^\circ\text{C}/\text{min}$  for all data collections. Midinfrared spectra were recorded on a Nicolet 800 FTIR spectrometer. Powder X-ray diffraction patterns were collected using a Scintag XDS 2000 diffractometer using Cu K- $\alpha$  radiation. The temperature-programmed X-ray diffraction sample measurements were performed on the same diffractometer using a Scintag high-temperature chamber equipped with a Pt–Rh alloy sample holder/strip heater. The chamber was connected to a dry argon flow. Glass transition and melting temperatures were obtained by differential scanning calorimetry (DSC) using a Perkin-Elmer DSC-7 with a heating rate of 10  $^\circ\text{C}/\text{min}$  under nitrogen flow. Electrochemical impedance data was obtained using a Solatron 1287 potentiostat/1260 frequency response analyzer. The composites were sandwiched between two platinum blocking electrodes and dried in situ in a Buchi oven under purging argon for at least 12 h prior to measurement. This was done so as to completely dehydrate the sample. Complete dehydration judged by sample mass loss over time was predetermined via an isothermal desorption experiment under flowing argon (see Figure S1 in the Supporting Information). Sample measurements were obtained during cooling by applying a 100 mV excitation voltage with a logarithmic frequency sweep from  $1 \times 10^{-1}$  Hz to  $1 \times 10^6$  Hz. Resistance values were taken at the minimum imaginary response in a  $Z'$  vs  $Z''$  plot to determine the conductivity in the low-frequency limit.

## Results and Discussion

**Stability of Bitriazole-PEO Composites.** Because strong adsorption of some NCHs poisons the platinum fuel cell catalysts,<sup>19</sup> it is important to assess the electrochemical stability of any new NCH under redox conditions. Electrochemical stability was probed by observing whether oxidative and/or reductive peaks appear in the presence of platinum over an electrochemical window of interest. Cyclic voltammograms (CVs) for bitriazole and imidazole in acetonitrile solutions purged with  $\text{O}_2$  are shown in Figure S2 of the Supporting Information. Unlike imidazole where a large irreversible oxidation peak appears after the first cycle near +1.3 V, bitriazole shows no observable redox peaks in the 0 to +1.8 V (vs Ag/AgCl) potential range, implying that bitriazole has sufficient electrochemical stability under fuel-cell operating conditions.

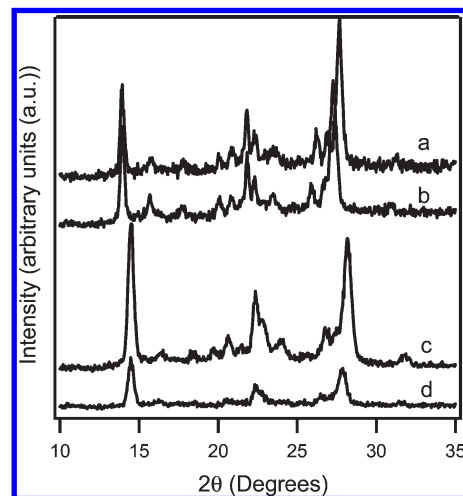


**Figure 1.** Powder XRD spectra of bitriazole at (a) 25 and (b) 150  $^\circ\text{C}$  and of bitriazole- $\text{PEO}_{1k}$  at (c) 25 and (d) 150  $^\circ\text{C}$ .

The hysteresis observed in the CV of bitriazole is due to electrode overpotential. Thermal analysis (see Figure S3 in the Supporting Information) shows that bitriazole appears stable up to 200  $^\circ\text{C}$ .

**Mobility in Bitriazole-PEO Composites.** When fully dried under anhydrous conditions, pristine bitriazole gives negligible conductivity ( $< 10^{-9}$  S  $\text{cm}^{-1}$ ) both at room temperature and 150  $^\circ\text{C}$ . The lack of proton conduction in pristine bitriazole is attributed to its densely packed hydrogen-bonded structure, as evidenced by the full retention of its crystalline structure after heat treatment to 150  $^\circ\text{C}$  (Figure 1). Because ethylene oxide based polymers are known to dramatically increase the conductivity of lithium ion salts via segmental motions of the ethylene oxide units and high dielectric constants,<sup>20</sup> we hypothesized that the conductivity in pristine bitriazoles could also be augmented in a similar fashion by mixing a poly(ethylene oxide) dimethyl ether ( $M_n \approx 1000$ ) ( $\text{PEO}_{1k}$ ) with bitriazole. A 20:1 bitriazole/ $\text{PEO}_{1k}$  ratio was chosen because this corresponds to a 1:1 ratio of the bitriazole molecule to the ethylene oxide monomer in  $\text{PEO}_{1k}$ . In addition, the structural integrity of the composite pellet was compromised at higher polymer fractions. The bitriazole- $\text{PEO}_{1k}$  composite, as shown by the representative TGA data (see Figure S3 in the Supporting Information), displays similar stability (up to 200  $^\circ\text{C}$ ) as pristine bitriazole.

The DSC data from pure  $\text{PEO}_{1k}$  and bitriazole- $\text{PEO}_{1k}$  are shown in Figure 2. The melt transition of  $\text{PEO}_{1k}$  at 32.5  $^\circ\text{C}$  is also observed in the bitriazole- $\text{PEO}_{1k}$  composite material, implying that some crystalline regions of  $\text{PEO}_{1k}$  are still present in the composite sample at room temperature. However, the degree of crystallinity is greatly reduced in the presence of bitriazole, as evidenced by the large reduction in the melting peak area. This large reduction in the  $\text{PEO}_{1k}$  crystallinity due to bitriazole incorporation should also lead to a decrease in the degree of bitriazole crystallinity as shown in Figure 1. Indeed, the powder XRD spectrum of bitriazole- $\text{PEO}_{1k}$  in contrast to

(19) Deng, W. Q.; Molinero, V.; Goddard, W. A. *J. Am. Chem. Soc.* **2004**, *126*(48), 15644–15645.

(20) Ratner, M. A.; Shriver, D. F. *Chem. Rev.* **1988**, *88*(1), 109–124.

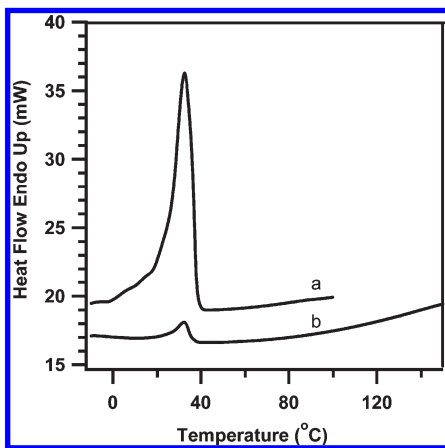


Figure 2. DSC curves of (a) PEO<sub>1k</sub> and (b) bitriazole-PEO<sub>1k</sub>.

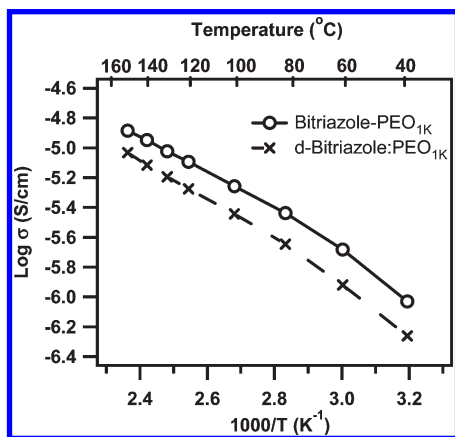


Figure 3. Conductivity data for bitriazole-PEO<sub>1k</sub> and deuterated-bitriazole-PEO<sub>1k</sub> at a 20:1 bitriazole/polymer ratio.

pristine bitriazole at 150 °C shows a decrease in the intensity of the reflections at 15.7, 20.1, and 20.9° while those at 17.9 and 23.6° are completely lost. This decline in the degree of bitriazole crystallinity signifies an increase in the formation of amorphous regions within the composite. The amorphous phase should be rich in polymer based on the large reduction in the semicrystallinity of PEO<sub>1k</sub>. Unlike pristine bitriazole, the crystallinity of bitriazole in the bitriazole-PEO<sub>1k</sub> composite decreases with increasing temperature (Figure 1). These results imply that the composition of the bitriazole in the amorphous, polymer rich phase increases with increasing temperature. Increasing the concentration of bitriazole in the PEO<sub>1k</sub> amorphous phase should facilitate proton mobility by way of segmental motion.

**Origin of Anhydrous Proton Conduction.** The conductivity of the bitriazole-PEO<sub>1k</sub> composite reached a maximum value of 13 μS/cm at 150 °C (Figure 3). This value is more than 4 orders of magnitude greater than the conductivity of pristine bitriazole ( $< 1 \times 10^{-9}$  S/cm). The origin of the proton conductivity was investigated by carrying out a kinetic isotope effect (K.I.E) experiment. To do this, isotopic substitution of the bitriazole amine protons with deuteriums was performed by contact with D<sub>2</sub>O. The substitution was confirmed via <sup>1</sup>H NMR by the complete disappearance of the broad bitriazole N–H

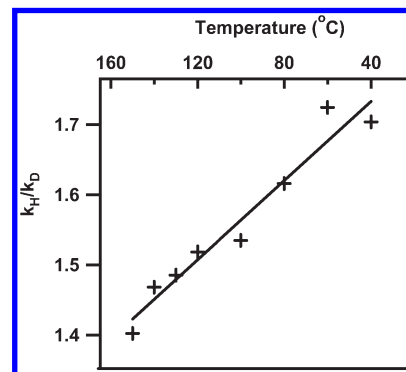


Figure 4.  $k_H/k_D$  (K.I.E) for bitriazole-PEO<sub>1k</sub> as a function of temperature.

peak centered at 15.2 ppm without a change in the C–H peak at 8.21 ppm (see Figure S4 in the Supporting Information). Further support for deuterium substitution was obtained from the FT-IR spectrum (see Figure S5 in the Supporting Information). A red shift of the hydrogen-bonded N–H stretching frequency between 2300 and 3000  $\text{cm}^{-1}$  to 1800 and 2400  $\text{cm}^{-1}$  (N–D) is observed because of the heavier deuterium atom. The C–H stretching frequency at  $\sim 3200$   $\text{cm}^{-1}$  remained constant in both samples, again confirming selective deuterium exchange at the bitriazole N–H site. The isotopic substitution results in a primary isotope effect shown by the data given in Figures 3 and 4. These data indicate that the N–H bond is involved in the rate-determining step of the proton conduction in the bitriazole-PEO<sub>1k</sub> composite. The ratio of the rate constants,  $k_H/k_D$ , increases as the temperature decreases (Figure 4) as expected, because of the larger effect of mass on ion motion at lower temperatures.

The theoretical maximum of  $k_H/k_D$  is 4.2 at room temperature, based on the full dissociation of the N–H bond in the transition state ( $\nu_H$  and  $\nu_D$  obtained from FT-IR data). However,  $k_H/k_D$  from the experimental data gives a value of  $\sim 1.7$ . The difference between the theoretical and experimental values suggests that proton transfer in the transition state does not involve the complete dissociation of N–H bonds.

**Effect of Polymer Concentration.** The bitriazole/PEO<sub>1k</sub> ratio was increased in order to investigate the effect of PEO<sub>1k</sub> content on conductivity. Composites with higher bitriazole fractions (40:1 and 100:1) had lower conductivities and greater temperature dependence. Lower conductivities can be attributed to a decrease in the polymer-rich phase in the composite as the fraction of bitriazole increases. The increase in temperature dependence implies a higher activation energy and stronger dependence on segmental motion. The slight curvature of the data in Figure 5 implies non-Arrhenius behavior, which is suggestive of coupling between polymer segmental motion and ion transport.<sup>10,21</sup> In proton conductive systems where polymers are involved with the charge carriers, conductivity depends not only on the number of charge

(21) Ratner, M. A., In *Polymer Electrolyte Reviews*; Elsevier Applied Science: New York, 1987; p 173.

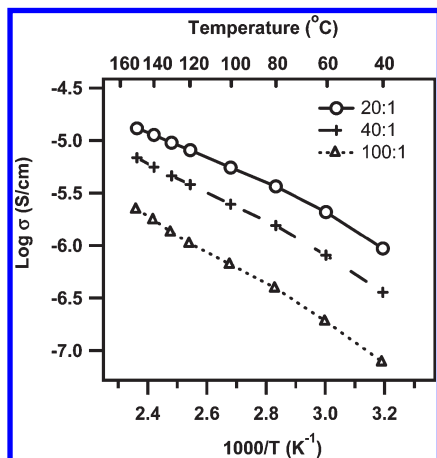


**Figure 5.** Conductivities of bitriazole-PEO<sub>1k</sub> composites with increasing bitriazole content.

**Table 2.** VTF Parameters Obtained from Fitting the Experimental Data in Figure 5 to eq 1

Bitriazole-PEG <sub>1k</sub>	$T_0$ (K)	$\sigma_0$ (S cm <sup>-1</sup> ) × 10 <sup>-3</sup>	$B$ (kJ/mol)	$R^2$
20:1	115.42	1.09	11.35	0.9999
40:1	122.82	1.02	12.55	0.9996
100:1	127.95	0.86	14.69	0.9988

carriers, their type, and mobility but also on the conformational changes in free volume. The temperature dependence on conductivity incorporating the latter has been described by the Vogel–Tamman–Fulcher (VTF) equation.<sup>21</sup>

$$\sigma = \sigma_0 e^{(-B/R(T-T_0))} \quad (1)$$

where  $\sigma_0$  correlates to the maximum number of mobile charge carriers in the system,  $B$  is an empirical parameter known as the Vogel activation energy, and  $T_0$  is widely described as the temperature at which all the free volume vanishes.  $T_0$  is usually 50–70 K below the glass transition temperature. The experimental data in Figure 5 were fit to the VTF model (eq 1) and the fitting parameters are summarized in Table 2.

The prefactor,  $\sigma_0$ , decreases as the fraction of bitriazole in the composite increases. Although there are more charge carriers in the composite, the experimental values obtained suggest that the number of charges available for proton conduction decreases. This observation is explained by the increase in  $T_0$ , as the bitriazole fraction increases. Because  $T_0$  has been shown to track with the  $T_g$ , its increase suggests a higher degree of rigidity in the composite as the bitriazole content increases. Thus, increasing bitriazole fraction in the range tested decreases the amount of polymer-rich regions, which leads to a decrease in overall segmental motion that results in a lower concentration of mobile bitriazole protons, hence the observed lower conductivities. Along the same line of reasoning, the Vogel activation energy,  $B$ , also increases (as expected) with increasing bitriazole fraction, indicating a higher energy conduction pathway. These results suggest that only the bitriazole protons associated with PEO<sub>1k</sub> in the amorphous phase participate in conductivity.

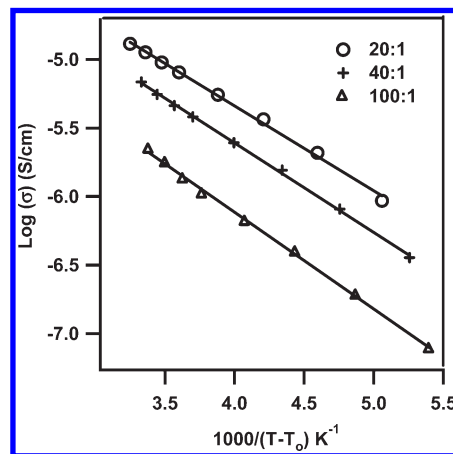


**Figure 6.** Conductivity as a function of the free volume normalized temperature ( $T - T_0$ ). Solid lines are generated from eq 1 using parameters from Table 2.

Complementary to these results, Goward et al. performed a comprehensive solid-state <sup>1</sup>H NMR study and found that proton transport in imidazole-terminated oligomers occurs almost exclusively in the amorphous disordered phase.<sup>22</sup> To verify the VTF behavior, the plot of  $\log(\sigma)$  should vary in a linear fashion with  $(T - T_0)^{-1}$ . This linear relationship is observed (Figure 6) for all three bitriazole/PEO<sub>1k</sub> ratios. The right shift of the linear conductivity plots in Figure 6 toward higher temperatures and lower conductivities as bitriazole content increases is the result of the increase in  $T_0$  as previously discussed. The slight increase in the slope, as reflected by the increase in  $B$ , with bitriazole content indicates that at higher temperatures (beyond 150 °C), the lines will converge. Because the free volume, and thus mobility, is less dependent on the polymer at higher temperatures, conductivity becomes more dependent on the number of charge carriers added. However, in the temperature window used here (25–150 °C), the mobility of the composite, as judged by the loss of bitriazole crystallinity in the powder XRD (Figure 1) and conductivity results, appears to be highly dependent on segmental polymer motion.

**Effect of PEO Length.** As an extension of the previous study, where increasing the bitriazole content decreased segmental mobility and thus conductivity, we expected the incorporation of higher molecular weight PEOs to lead to a decrease in mobility and proton conductivity. Because higher molecular weight PEOs were not available, high molecular weight ( $M_n = 4000$  and  $8000$ ) poly(ethylene glycols) (PEGs), i.e., with terminal hydroxyl groups, were employed. To investigate the effect of the terminal hydroxyl end groups, we compared conductivities of bitriazole-PEG<sub>1k</sub> to the bitriazole-PEO<sub>1k</sub> composites (both at a 20:1 bitriazole/PEO<sub>1k</sub> ratio). As shown by the data in Figure 7, the terminal hydroxyl groups do not have a significant effect on proton conductivity. The bitriazole/PEG<sub>4k</sub> and bitriazole/PEG<sub>8k</sub> ratios were adjusted to 80:1 and 160:1 in order to maintain a 1:1 ratio of bitriazole to ethylene oxide unit within each composite. In

(22) Goward, G. R.; Schuster, M. F. H.; Sebastiani, D.; Schnell, I.; Spiess, H. W. *J. Phys. Chem. B* **2002**, *106*(36), 9322–9334.

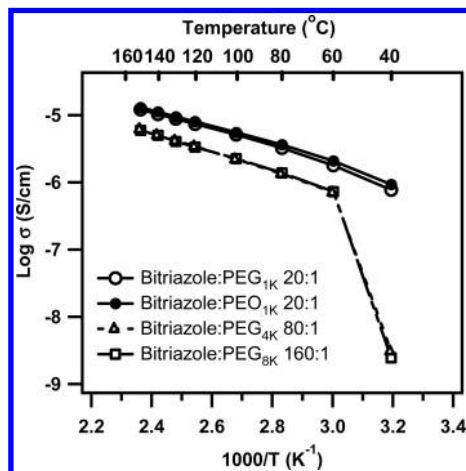


Figure 7. Effect of PEO length on conductivities.

contrast to the bitriazole- $\text{PEG}_{1k}$  composite, the conductivities of bitriazole composites with  $\text{PEG}_{4k}$  and  $\text{PEG}_{8k}$  undergo a sudden drop below 60 °C. The drop in conductivity is similar for both compounds because all high molecular weight PEGs ( $M_n > 4000$ ) have similar melt temperatures of 59–61 °C. Below this temperature, these high molecular weight PEGs form crystalline regions, which lack mobility and thus lead to a sharp decline in conductivity. Above their melt temperature, the conductivities of bitriazole- $\text{PEG}_{4k}$  and bitriazole- $\text{PEG}_{8k}$  are lower than that of the bitriazole- $\text{PEG}_{1k}$  because of their lower mobility. However, the bitriazole- $\text{PEG}_{4k}$  and  $\text{PEG}_{8k}$  composites appear to have no appreciable difference in their conductivities. These data appear to suggest that above a certain PEG molecular weight ( $M_n = 4000$ ), the differences in mobility with respect to their influence on proton conductivity is diminished.

**Effect of Acid Groups Tethered onto  $\text{PEO}_{1k}$ .** Proton conductivity in NCHs has been shown to increase with the addition of strong acid dopants, such as trifluoroacetic acid (TFA), methane sulfonic acid (MSA), or paratoluenesulfonic acid (pTSA). These small-molecule acids have  $pK_a$  values lower than the basic  $pK_a$  of most NCHs, and are thus able to protonate the basic sites and lead to an increase in the concentration of charge carriers. However, direct addition of these small molecules introduces the possibility of proton vehicular transport. Also, incorporation of these acids into the bitriazole- $\text{PEO}_{1k}$  composite gives a significant reduction in the mechanical integrity of the composite structure. To circumvent this problem, we tethered the acidic dopants of different acid strength to the terminal ends of the PEO. This allowed for the study of the influence of the strength of acid dopants on proton diffusion in bitriazole- $\text{PEO}_{1k}$  composites. The terminal hydroxyl groups in  $\text{PEG}_{1k}$  were shown to have negligible effects on the proton conductivity (Figure 7). For an acidic group to protonate the bitriazole, its  $pK_a$  must be comparable to or lower than the basic  $pK_a$  of bitriazole (−1, Table 1). As shown in Figure 8, both terminal alcohols and carboxylic acids are not able to significantly affect the composites because their  $pK_a$ 's ( $\sim 15.2$  and  $\sim 4.8$ , respectively) are higher than the basic

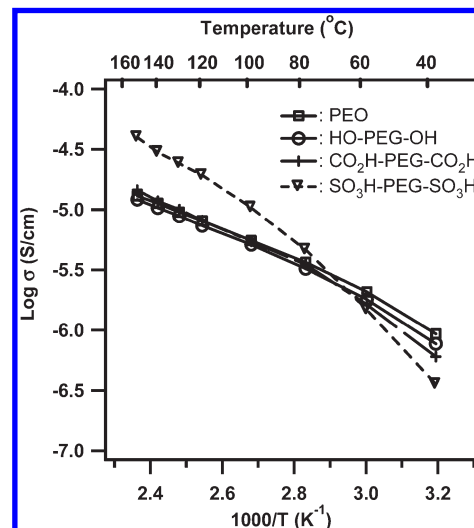


Figure 8. Influence of acid type on proton conductivity. The composites were prepared at a 20:1 bitriazole/PEO-acid ratio (9 mol % acid groups).

$pK_a$  of bitriazole. The lack of an appreciable increase in proton conductivity of the bitriazole-PEO-dicarboxylic acid composite ( $\text{COO-H } pK_a 4.8$  vs bitriazole- $H$   $pK_a 6.4$ ) implies a structural diffusion pathway of proton conduction via the bitriazole molecules. The PEO-disulfonic acid with a  $pK_a$  of approximately −2 gives a 3-fold increase in proton conductivity at 150 °C. This increase is consistent with literature values that report about an order of magnitude increase in conductivity with small-molecule dopant concentrations of 5–15%.<sup>9,11</sup> The additional 3-fold increase in literature may be due to contributions from the vehicular transport of the small molecule acid groups used. The conductivity of the bitriazole-PEG-disulfonic acid shows greater temperature dependence than the undoped composite and its conductivity falls below that of  $\text{PEO}_{1k}$  at low temperatures. The lower conductivity at low temperatures could be due to a higher  $T_g$  of the polymer because of the introduction of the terminal sulfonic acids that are able to electrostatically interact with the bitriazole. A lower  $T_g$  will lead to a stiffer polymeric system, thus leading to the higher temperature dependence observed.

**Effect of Polymer Type.** The synergistic effect between bitriazole and the PEOs was investigated by altering the type of flexible polymer and measuring the proton conductivity. If conductivity is governed solely by conformational free-volume changes in the polymer, then a different polymer with similar molecular weight and flexibility, such as polypropylene glycol (PPG,  $M_n \approx 1000$ ), should give comparable conductivity results.  $\text{PPG}_{1k}$ , unlike  $\text{PEG}_{1k}$ , is an amorphous polymer (no melt transition) and has a similar  $T_g$  to  $\text{PEG}_{1k}$  (ca. −70 °C).<sup>23,24</sup> In theory,  $\text{PPG}_{1k}$  should be just as flexible (if not more) as  $\text{PEG}_{1k}$ . A bitriazole- $\text{PPG}_{1k}$  composite was prepared at a 16:1 ratio in order to maintain a 1:1 bitriazole/propylene oxide ratio.

(23) Jeong, Y. G.; Pagodina, N. V.; Jiang, C.; Hsu, S. L.; Paul, C. W. *Macromolecules* **2006**, *39*(14), 4907–4913.

(24) Park, J. T.; Lee, K. J.; Kang, M. S.; Kang, Y. S.; Kim, J. H. *J. Appl. Polym. Sci.* **2007**, *106*(6), 4083–4090.

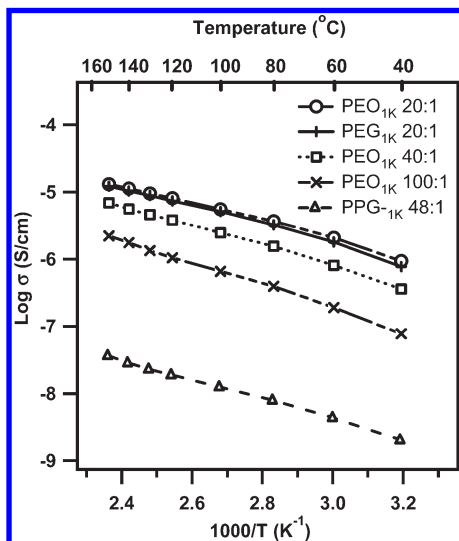


**Figure 9.** Conductivities of bitriazole-PEO, -PEG, and -PPG composites. All polymers have a  $M_n \approx 1000$ .

The bitriazole to polymer ratio in all the composites was confirmed by  $^1\text{H}$  NMR, after conductivity experiments, to be the same as the initial loading. However, with  $\text{PPG}_{1k}$ , leaching was observed during composite preparation, suggestive of poor incorporation of the  $\text{PPG}_{1k}$  polymer in the composite.  $^1\text{H}$  NMR after the conductivity experiment gave a 48:1 bitriazole/ $\text{PPG}_{1k}$  ratio as reported in Figure 9. The conductivity of the bitriazole- $\text{PPG}_{1k}$  composite is over 2 orders of magnitude lower than the 40:1 or even the 100:1 bitriazole- $\text{PEO}_{1k}$  composites. This significant difference in conductivity indicates that the conductivity enhancement observed in the bitriazole- $\text{PEO}_{1k}$  composites is not a sole function of segmental motion. In addition, the difference highlights the importance of the ethylene oxide group and suggests a cooperative interaction between the ethylene oxides and the bitriazole proton. Because ethylene oxides are known to be excellent cationic chelators because of their electron-donating properties, these groups may promote proton conduction within the amorphous regions in the bitriazole-PEO composites by interrupting the strong hydrogen bonds between the bitriazole molecules. This specific chelate interaction is absent in the bitriazole- $\text{PPG}_{1k}$  composite, possibly because of the presence of the extra methyl group, which deters association with the bitriazole proton either via hydrophobicity or steric hindrance. One can also not rule out the possibility that the higher dielectric constant of  $\text{PEO}_{1k}$  over  $\text{PPG}_{1k}$  may play a significant role in fostering a highly polar environment for proton transport.

**Synergy between Bitriazole and  $\text{PEO}_{1k}$ .** In an effort to probe and understand the synergistic effects between bitriazole and the ethylene oxides in bitriazole-PEO composites, we used solid- and liquid-state  $^1\text{H}$  NMR techniques to obtain information on structural properties. Both the solid- and liquid-state  $^1\text{H}$  NMRs of bitriazole and its  $\text{PEO}_{1k}$  composite are almost identical, as expected (see Figure S4 in the Supporting Information). In the liquid  $^1\text{H}$  NMR, the C-H proton appeared at 8.21 ppm as a sharp singlet, whereas the N-H proton appeared

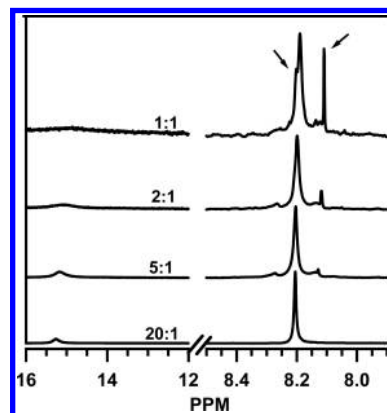


**Figure 10.**  $^1\text{H}$  NMR in  $\text{DMSO-}d_6$  of bitriazole- $\text{PEO}_{1k}$  with increasing  $\text{PEO}_{1k}$  fraction from 20:1 to 1:1. Arrow indicates the new peaks at 8.11 and 8.20 ppm.  $\text{PEO}_{1k}$  peaks appear at 3–4 ppm (not shown).

further downfield at 15.26 ppm as a broad averaged singlet. The  $^1\text{H}$  NMR of bitriazole- $\text{PEO}_{1k}$  (20:1) composite, both in the liquid and solid state, looks like a superimposition of bitriazole and  $\text{PEO}_{1k}$  (not shown)  $^1\text{H}$  NMR spectra, i.e., no new peaks or shifts was observed. However, in the liquid-state NMR, when the ratio of bitriazole to  $\text{PEO}_{1k}$  is decreased from a 20:1 to 1:1 ratio, two new peaks at 8.11 and 8.20 ppm arise, as shown in Figure 10. As the fraction of  $\text{PEO}_{1k}$  increases, the intensity of the 8.11 and 8.21 ppm peaks increase and the intensity of the N-H peak at 15.3 ppm decreases. This proton is associated with the nitrogen atom on the bitriazole (the proton signal disappears in  $\text{D}_2\text{O}$  due to rapid exchange). The upfield N-H shift is suspected to be due to interruption of the strong intermolecular hydrogen bonds between bitriazole molecules by the ethylene oxides in  $\text{PEO}_{1k}$ , which are known to form complexes with metal cations in solution. The hydrogen bonds formed between the ethylene oxides of  $\text{PEO}_{1k}$  and the N-H of the bitriazole, i.e.,  $\text{N-H}\cdots\text{O}$ , are weaker ( $\sim 1.9$  kcal/mol) than those between two bitriazoles, i.e.,  $\text{N-H}\cdots\text{N}$  ( $\sim 3.1$  kcal/mol).<sup>25</sup> The weaker hydrogen bonded bitriazole protons appear upfield from their strongly bound counterparts. These new peaks are observed only at high  $\text{PEO}_{1k}$  concentrations. Thus, it appears that multiple ethylene oxides are required to interrupt the strong hydrogen bonds between bitriazole molecules. These results complement those of Marcella Iannuzzi who showed via molecular dynamics simulations (meta-dynamics approach) that neighboring oxygen atoms in Imi-2EO (two imidazole molecules linked by a diethylene glycol spacer) stabilize the proton migration steps via  $\text{O}\cdots\text{H}$  interactions.<sup>26</sup>

The 8.11 and 8.20 ppm N-H protons are not observed in the solid-state NMR because of the broad signals (see Figure S4 in the Supporting Information) and low concentrations. To investigate the possible role of these N-H protons in the conductivity, we carried out liquid-state NMR of bitriazole- $\text{PPG}_{1k}$  at a 1:1 ratio for comparison. The 8.11 and 8.21 ppm protons are absent in the bitriazole- $\text{PPG}_{1k}$  1:1 complexes

(25) Emsley, J. *Chem. Soc. Rev.* **1980**, 9(1), 91–124.

(26) Iannuzzi, M. *J. Chem. Phys.* **2006**, 124, 204710.

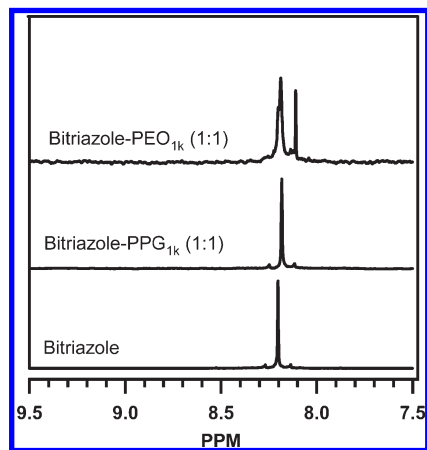


**Figure 11.**  $^1\text{H}$  NMR of bitriazole, bitriazole-PPG<sub>1k</sub> (1:1), and bitriazole-PEO<sub>1k</sub> (1:1) in DMSO-*d*<sub>6</sub>.

(Figure 11). This is most likely due to steric destabilization as a result of the extra methyl group in propylene oxide, which may also be the reason for the observed poor proton conductivity (Figure 9). We believe that the 8.11 and 8.20 ppm protons observed in Figures 10 and 11 are also present in the solid state, albeit at very low concentrations, and these protons are responsible for the appearance of the observed proton conductivity. This can be rationalized by examining the way the composite materials were created. The composite is prepared via evaporation of a methanol solution containing both dissolved bitriazole and PEO<sub>1k</sub> in a 20:1 ratio. As the methanol slowly evaporates, small precipitates begin to form from the saturated solution. Because the solubility of the PEO<sub>1k</sub> in methanol is much higher than in bitriazole, and bitriazole is present in excess, the fraction of bitriazole molecules in the primary precipitates must be much higher than 20:1. Further along the evaporation, this ratio decreases and a polymer-rich phase is obtained. Thus, although mixed at a 20:1 ratio, the composite material should contain bitriazole-rich regions, as well as PEO<sub>1k</sub>-rich regions with bitriazole-PEO<sub>1k</sub> ratios approaching or exceeding 1:1 in the polymer-rich amorphous regions. The latter, though present in small amounts, is responsible for the proton conductivity observed in the bitriazole-PEO<sub>1k</sub> (20:1) composite.

### Conclusions

The proton conductive pathway in the bitriazole-PEO<sub>1k</sub> composite is proposed to involve three key steps. The first is the formation of an amorphous polymer-rich

bitriazole phase due to positive interactions between the ethylene oxides in PEO<sub>1k</sub> and the bitriazole proton. This phase is created within a crystalline bitriazole network, which provides the structural mechanical integrity for the composite. Second, the mobility of the polymer increases with temperature and induces segmental motion into the polymer-rich bitriazole phase, which contains bitriazole molecules associated possibly via weak hydrogen bonds to the ethylene oxides in PEO<sub>1k</sub>. The protons being transferred most likely arise from intra- or intermolecular autoprotolysis of bitriazole (defect sites), similar to that in water. Third, segmental motion as a result of the PEO<sub>1k</sub> leads to significant local dynamics, which foster proton transfer via structural diffusion from one mobile bitriazole molecule to the next because of their amphoteric nature. Triazoles unlike imidazoles are tautomeric and can thus undergo intramolecular 1,2 prototropic shifts from the N3 (*C<sub>s</sub>*) to the N2 (*C<sub>v</sub>*) position.<sup>27</sup> Thus, with bitriazoles, there is the possibility of intramolecular proton transfer between the two triazole rings in the transition state. On the basis of the data from the KIE experiment, the proton is not fully dissociated in the transition state but probably bridges between two nitrogen atoms.

Overall, this work presents several results confirming the concept of anhydrous proton conductivity via structural diffusion of the bitriazole proton in a polymer-rich region within a crystalline nonconductive bitriazole framework. A rich amorphous phase with high segmental mobility is essential, along with ethylene oxide groups, which increase the amount of available protons via positive interactions with the NCH. In addition, acidic groups with *pK<sub>a</sub>* values lower than the basic *pK<sub>a</sub>* of the NCH are crucial to obtaining higher conductivities at elevated temperatures. These conclusions provide valuable information for further design and development of polymeric NCHs as polymer electrolyte membranes for fuel cell and other electrolyte applications.

**Acknowledgment.** This work was supported by the DOE (DE-FG02-05ER15716).

**Supporting Information Available:** Experimental details, TGA, CV, FT-IR and NMR data (Figures S1–S5) (PDF). This material is available free of charge via the Internet at <http://pubs.acs.org>.

(27) Lunazzi, L.; Parisi, F.; Macciantelli, D. *J. Chem. Soc., Perkin Trans. 2* **1984**, 6, 1025–1028.